

Phase Behavior of Ultrathin Polymer Mixtures

Ronald L. Jones,[†] Ananth Indrakanti,[‡]
Robert M. Briber,[§] Marcus Müller,[⊥] and
Sanat K. Kumar^{*,*||}

Department of Materials Science and Engineering and
Department of Chemical Engineering, The Pennsylvania
State University, University Park, Pennsylvania 16802,
Department of Nuclear and Materials Engineering,
University of Maryland, College Park, Maryland,
Department of Physics, Johannes Gutenberg Universität,
Mainz, Germany, and Department of Chemical Engineering,
Rensselaer Polytechnic Institute, Troy, New York 12180

Received May 6, 2004

Revised Manuscript Received July 2, 2004

Existing equilibrium theories and simulations uniformly suggest that confinement should dramatically affect the location of the liquid–liquid-phase transition temperature of polymer blends.^{1–3} In apparent agreement with these ideas previous light scattering measurements^{4,5} suggest that $|T_{c,D} - T_{c,bulk}| \approx 50$ K can be obtained for $D \approx 100$ nm. These conclusions are not in agreement with scattering measurements on filled polymer blends,^{6–8} which show that the binodal temperature is hardly shifted on confinement. These newer findings on filled systems receive indirect support from measurements of the temperature, T_R , at which the air surface of a blend film roughens.⁹ This temperature has been conjectured to be the thin film binodal. Limited data on T_R 's for films of seven different polymer blends are roughly equal to their respective bulk binodals, consistent with results on the filled systems.^{10–15} While a number of recent experiments appear to be reaching a consensus that the binodal temperature is hardly affected on confinement, there are two separate issues here. First, the experiments, in each case, are indirect measures of confined phase behavior. Second, it is clear that the existing equilibrium theory and the new experiments are in qualitative disagreement.

To obtain direct estimates of phase behavior here we present small-angle neutron scattering (SANS) measurements of thin film phase diagrams of two model blends (Table 1). SANS, which typically utilizes neutrons with wavelengths in the 5–15 Å range, is particularly advantageous over light scattering since it is sensitive to the onset of phase separation. Our results assert the disagreement between theory and experiments and show that, even though the critical composition is shifted from its bulk value for films as thick as 600 nm, the thin film binodal temperatures are always within 8 K of their bulk values. We have carefully considered and ruled out all equilibrium possibilities that we could imagine to explain this discrepancy between existing theories and experiments.¹⁶ Consequently, we are forced to conclude that the experiments are dominated by the well documented fact that polymer chains placed on wettable substrates are effectively ir-

reversibly adsorbed, e.g., refs 17–27. In the filled rubber community, these slowly relaxing, effectively irreversibly adsorbed, chains are termed as a “bound” polymer layer.^{28,29} Supported by computer simulations, we suggest that, at adsorbing boundaries, the blends create their own “surfaces” comprised of bound chains. We therefore propose that since such bound layers can be wetting autophobic,^{30,31} polymer blends in their vicinity act as though they were next to a weakly attractive boundary and phase separate near their bulk binodal.

A series of films of the deuterated poly(butadiene)/poly(1,4-isoprene) [dPB/hPI] blend of thickness $60 \text{ nm} \leq D \leq 1 \text{ } \mu\text{m}$ were spin-cast from toluene solution onto polished silicon wafers which were pre-cleaned using a boiling bath of $\text{H}_2\text{O}/\text{NH}_3/\text{H}_2\text{O}_2$ (5:1:1 by volume), followed by a heated bath of 70% H_2SO_4 /30% H_2O_2 . This procedure preserves the native silicon oxide layer. For the deuterated poly(methylbutylene)/poly(ethylbutylene) [dPMB/hPEB] blend, we etched the substrate with 2 wt % HF to remove the native oxide layer. We used these different surfaces since they, respectively, were the ones that were wet by both blend components in each case. Film thicknesses were measured by ellipsometry. Bulk samples ($D \approx 1$ mm) were cast from toluene and pressed between quartz plates. The transmission SANS experiments were conducted in a vacuum, after annealing for 2–8 h at each temperature, using $\lambda = 8$ Å neutrons. (For more details on the scattering experiments, see ref 32.) The resulting data were first analyzed using the Ornstein–Zernike form, and this interpretation was confirmed by using the random phase approximation (RPA). The Flory interaction parameter, χ , and the R_G 's of the two species are the unknowns obtained by fitting the RPA to the experimental data.^{33,34} It is important to note that, although the RPA was developed for three-dimensional systems, past work has shown that it can be reliably used to interpret SANS data on films as thin as $D = 2R_G$ ^{35,36} at least over the limited range $qR_G \leq 5$.

We first consider bulk phase behavior. The dPB/hPI blend phase separates on heating, while the dPMB/hPEB blend phase separates on cooling. RPA analysis of the SANS experiments yields estimates for the forward scattering intensity, $I(0)$. Following standard practice the spinodal temperature, T_s , is estimated by a linear extrapolation of $1/I(0)$ vs $1/T$ to $1/I(0) = 0$. For the critical composition, ϕ_c , we obtain linear plots of $1/I(0)$ vs $1/T$ (Figure 1 insets). References 37 and 38 have shown that off-critical blends demonstrate a “kink” in plots of $1/I(0)$ vs $1/T$: this kink occurs at the point where the sample *actually* phase separates through a nucleation and growth mechanism (“cloud” point). The break in $1/I(0)$ is thus identified as the cloud point, T_{cl} .³⁸ Data for temperatures on the one-phase side of this break are extrapolated to $1/I(0) = 0$ to obtain the T_s . Note that we do not find any “breaks” in the dPMB/hPEB data because the bulk binodals, as predicted by the Flory–Huggins theory (see Figure 1b), were not crossed in the experiment for any of the compositions considered. The RPA also yields estimates for the Flory χ parameter³⁹ in the miscible regime. We find χ to be independent of ϕ over the range $0.25 \leq \phi \leq 0.75$ for dPB/hPI and $0.2 \leq \phi \leq 0.5$ for dPMB/hPEB. The bulk binodal and spinodal temperatures calculated using the Flory–Huggins model with these χ values are consistent with the T_{cl} and the

* Corresponding author. E-mail: kumar@rpi.edu.

[†] Department of Materials Science and Engineering, The Pennsylvania State University.

[‡] Department of Chemical Engineering, The Pennsylvania State University.

[§] University of Maryland.

[⊥] Johannes Gutenberg Universität.

^{||} Rensselaer Polytechnic Institute.

Table 1. Parameters for the Systems Studied

component	M_n	M_w/M_n	source	T_c , °C	ϕ_c	χ
dPB ^a	104 000	1.06	Polymer Source	50	$\phi_{dPB} = 0.65$	$-1.25 \times 10^{-2}/T + 5.2 \times 10^{-5}$
hPI ^b	144 000	1.03	Polymer Source			
dPMB ^c	180 000	1.07	N. Balsara	7	$\phi_{dPMB} = 0.32$	$1.19 \times 10^{-2}/T - 3.0 \times 10^{-5}$
hPEB ^d	48 000	1.07	N. Balsara			

^a Deuterated poly(butadiene). ^b Poly(1,4-isoprene). ^c Deuterated poly(methylbutylene). ^d Poly(ethylbutylene).

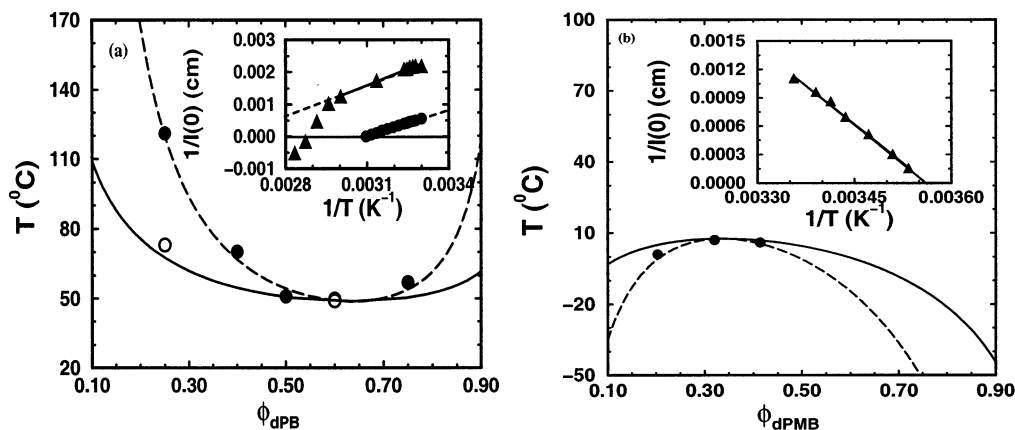


Figure 1. Bulk phase diagram for both blends. Plotted are SANS data for the spinodal (solid circles) and the binodal (open circles) temperatures as a function of ϕ . The solid and dashed lines are the predictions for the binodal and spinodal, respectively, from the Flory–Huggins theory. Insets: $1/I(0)$ plotted as a function of $1/T$ for (a) dPB/hPI blend and (b) dPMB/hPEB blend. The inset in part a shows plots for the bulk critical composition, $\phi_{dPB} = 0.60$ (solid circles), and an off-critical composition, $\phi_{dPB} = 0.40$ (solid triangles). The inset in part b shows the plot for a near-critical composition of the bulk, $\phi_{dPMB} = 0.316$ (solid triangles). Linear fits used to estimate the spinodal temperature are shown for both samples (line).

extrapolated T_s values at each ϕ (see Figure 1). Similarly, our T_s estimates for the dPMB/hPEB blend match the Flory predictions.

We now consider the thin film samples. While we have examined three different compositions for each blend, here we shall only consider films at the bulk critical concentration in detail. Neutron reflectivity (NR) experiments clearly show that the hPI from dPB/hPI blends, and the dPMB from the dPMB/hPEB blends are segregated to both the air and the Si surfaces (“symmetric” segregation).^{10,15} The RPA analysis of SANS data yields $\xi_{\parallel}^2 = \sigma^2 I(0)/[18\phi(1-\phi)k_N]$, where k_N is the neutron contrast, σ is the average Kuhn segment length³⁴ of the chains, and ϕ is the bulk composition. We denote the correlation length as ξ_{\parallel} since the SANS experiments have a scattering vector, and hence sensitivity, primarily parallel to the surfaces. Figure 2 shows that ξ_{\parallel} is suppressed relative to its bulk value for $D \leq 0.5 \mu\text{m}$, i.e., for $D \leq 10\xi_{\parallel}^{\text{bulk}}$, for the dPB/hPI blend. For $D \rightarrow 0$, $\xi_{\parallel}/D \sim 0.1$ at all temperatures. Similar results are found for the dPMB/hPEB blend, although the range of D values considered is much smaller (inset to Figure 2). The ξ_{\parallel} values for the dPB/hPI blend are compared to results obtained from NR.¹⁴ NR is primarily sensitive to composition profiles perpendicular to the surface (not concentration fluctuations) and thus provides complementary information to the SANS. NR indicates that the correlation length, ξ_{\perp} , obtained from the equation: $\int_0^D \phi^2(z) dz = 2\xi_{\perp}^2$, where ϕ_m is the composition in the middle, is strongly dependent on thickness. The equality results from assuming a form $\phi(z) \propto \exp(-z/\xi_{\perp})$ for the z -dependent concentration profile $\phi(z)$, and experimentally derived values of ξ_{\perp} are listed in refs 14 and 15. Figure 2 shows that the ξ_{\perp} track the ξ_{\parallel} obtained from SANS, to within a factor of 2 in all cases.

The SANS data also suggest that the magnitude of concentration fluctuations, as reflected in $I(0)$, are suppressed over the same D values (Figure 3). We extrapolate the $1/I(0)$ data to the limit of $1/I(0) = 0$ to

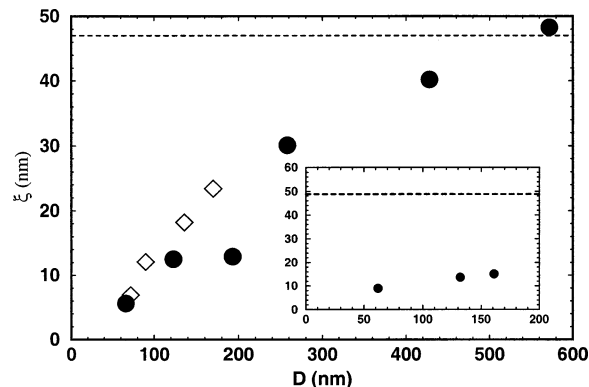


Figure 2. dPB/hPI blend ($\phi_{dPB} = 0.60$). Correlation length derived from SANS, ξ_{\parallel} , as a function of D at $T = 49$ °C (solid circles). Also shown are data for ξ_{\perp} reported by Grull at the same temperature (open diamonds). Inset: corresponding information for the ξ_{\parallel} from SANS for the dPMB/hPEB blend ($\phi_{dPMB} = 0.316$) at $T = 10$ °C. In both cases the dashed horizontal line corresponds to the bulk correlation length, $\xi_{\parallel}^{\text{bulk}}$.

obtain the extrapolated spinodal temperature, T_s . Self-consistent mean-field calculations on thin films using the Landau–Ginzburg free energy functional suggest that such an extrapolation does yield a proper estimate of the spinodal temperature even for thin films. At each D , the $1/I(0)$ vs $1/T$ plots have a minimum, for example at $1/T = 3.18 \times 10^{-3} \text{ K}^{-1}$ for $D = 480 \text{ nm}$ (see Figure 3a). These blends, which correspond to the bulk critical composition, are thus off-critical even for films as thick as $D = 600 \text{ nm}$ for the dPB/hPI blend. This is a direct consequence of surface segregation effects as shown recently by Budkowski et al.⁴⁰ We extrapolate the $1/I(0)$ data on the one phase side of this kink to the limit $1/I(0) = 0$ to obtain T_s . Our extrapolations consistently show $T_{s,D} = T_{c, \text{bulk}} \pm 3 \text{ K}$ for $D \geq 250 \text{ nm}$, i.e., no change in T_s within experimental uncertainty. For $D < 250 \text{ nm}$ (dPB/hPI), we linearly extrapolate only the five lowest temperature points due to strong curvature in the data. Consistent with the significant decrease in scattering

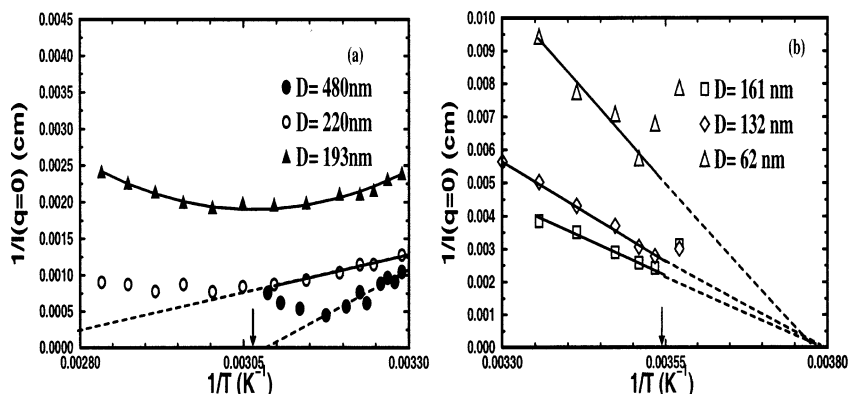


Figure 3. $1/I(0)$ is plotted vs $1/T$ for both blends. Also shown are the linear extrapolations to the spinodal temperatures (dashed lines). (a) dPB/hPI blend. For the two thicker films the cloud points were obtained by locating kinks in the curve. For the thinnest film the cloud point was determined by fitting a parabola to the data (solid line) and identifying the temperature corresponding to the maximum intensity (shown by the solid arrow). (b) dPMB/hPEB blend. The cloud points were identified by locating kinks in the curves. The solid arrow represents the bulk binodal/spinodal temperature.

with decreasing D , the T_s values for thinner films are substantially higher than $T_{c,\text{bulk}}$. For $D = 123$ nm, the $T_s = 453$ K ($T_s - T_{c,\text{bulk}} \approx 130$ K; see Figure 4a). Interestingly, the apparent shifts in T_s for the dPMB/hPEB blend are much smaller, ~ 20 – 50 K for all thicknesses and compositions considered. The expected statistical error in T_s is 10–15 K, as obtained from the Ornstein–Zernike fits. Note that the shifts in T_s are larger for $\phi_{\text{dPMB}} < \phi_{c,\text{bulk}}$, where $\phi_{c,\text{bulk}}$ is the bulk critical composition of the dPMB/hPEB blend. Also, for $\phi_{\text{dPMB}} = 0.414$ and 0.203 , the T_s shifts become stronger as D decreases. These results are consistent with the theoretical predictions for the phase boundary as a function of film thickness and composition.⁴¹ In combination, these results show conclusively that concentration fluctuations are suppressed on confinement over a broad range of D and that the extrapolated spinodals are predicted to be shifted outside error on confinement.

Following the past work of Schwahn^{37,38} on bulk polymer mixtures, we identify the kinks in the $1/I(0)$ vs $1/T$ plots (Figure 3) as the actual phase separation temperatures, or cloud points, of these films, T_{cld} . Though not investigated systematically, previous AFM and optical microscopy work on thin polymer films is consistent with the fact that the air surfaces of these films, which are smooth in the single phase state, roughen when the thin film binodal is crossed.^{10–13,15,42} Our thin films also show similar roughening of the air surface in the vicinity (± 8 K) of the “kink” temperatures in Figure 3. Moreover, close to the “kink” temperatures, Kratky plots ($q^2 I(q)$ vs q) start showing an upturn at very low q indicating the formation of sharp interfaces. These facts, in combination, provide credence to our assignment of T_{cld} to the “kink” in the scattering curves. Though there are errors involved in such an assignment, they are less than the statistical errors in the $I(0)$ values for various temperatures. While the kink is clear for all thick dPB/hPI films and for all the dPMB/hPEB films, the data are much more rounded for dPB/hPI films with $D \leq 250$ nm. To be consistent with the thickest films, the T_{cld} is estimated as the temperature with maximum $I(0)$ by using a parabolic fit to the data. Figure 4a shows that $T_{\text{cld}} = T_{c,\text{bulk}} \pm 8$ K for $58 \text{ nm} \leq D \leq 1 \mu\text{m}$ for both blends.

To summarize: our experimental results for the extrapolated spinodals are consistent with theory in that a significant stabilization of the single phase is predicted. However, the apparent thickness independence of the binodal as obtained from thin film SANS, from the AFM estimates of the roughening temperature of

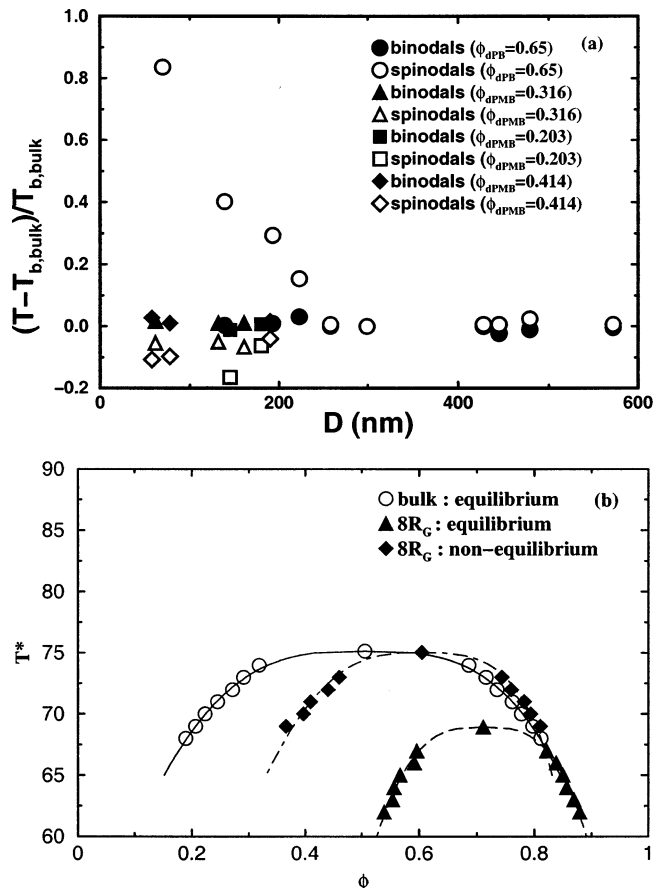


Figure 4. (a) Cloud point (solid symbols) and spinodal temperatures (open symbols) as a function of film thickness, D , for the dPB/hPI and dPMB/hPEB blends, respectively. The detailed legend is provided in the figure. Note that the spinodal shifts on confinement for both systems suggest a stabilization of the single phase in agreement with theory. The absolute signs of the shifts for the two systems take on opposite values since one blend phase separates on heating, while the other phase separates on cooling. (b) Phase diagrams as obtained from Monte Carlo simulations of a binary polymer blend in the bulk as well as in an $8R_G$ thick film confined between two identical surfaces. Model parameters are mentioned in the text. The nonequilibrium results for the $8R_G$ thick film are obtained by including an immobile $0.5R_G$ thick layer of the preferred component at each surface.

seven different blends,^{10–13,15,42} and from scattering measurements on filled polymer blends^{6–8} is in disagreement with theory. Analytical approximations in

theories appear to not be the source of these discrepancies since computer simulations, which are exact for any chosen model, do not reproduce the experimental trends. It is clear that there is a critical aspect of the experimental situations which has been missed in the current analysis. After considering all equilibrium scenarios we could imagine, we are forced to conclude that this variable is the effectively irreversible adsorption of the polymer chains onto the substrate.^{17,19–23}

To understand the role of these adsorbed layers on phase behavior we performed Monte Carlo simulations for lattice polymer blends of chain length $N = 100$. We considered a symmetric polymer blend with the following nearest neighbor interaction parameters: $\epsilon_{AA} = \epsilon_{BB} = -1$, $\epsilon_{AB} = \epsilon_{hh} = \epsilon_{hA} = \epsilon_{hB} = 0$, where h denotes an empty lattice site and A and B are the two blend components. The blend is sandwiched between two identical surfaces separated by $8R_G$ ($R_G \approx 5.3$ lattice units). The energetic interactions with the surface are short-ranged and described by $\epsilon_{As} = -200$, $\epsilon_{Bs} = -100$ and $\epsilon_{hs} = 0$. Temperature is defined as $T^* = k_B T / |\epsilon_{AA}|$. For the nonequilibrium simulation, a $0.5R_G$ thick layer of the preferred component (A) is irreversibly (and randomly) adsorbed at each surface. In the course of the simulation, the segments in contact with the surfaces are not allowed to move. Figure 4b shows the phase diagram for the bulk system and the thin film with and without (equilibrium) the grafted layers. We find that, in the presence of irreversibly pinned layers, the blend phase separates very close to the bulk binodal temperature. Note also that the critical composition is altered as in the experiments, primarily due to the presence of the adsorbed layers. While we cannot be conclusive, we speculate that these results are a consequence of the fact that melt chains have a propensity to autophobically dewet the “pinned” polymer layers.^{30,43–45} Thus, the matrix chains (i.e., all chains except the pinned chains) act as though they were in the vicinity of a weakly attractive surface and phase separate roughly at their bulk values. We emphasize here that we have had to evoke relatively new physics to allow us to reconcile our experimental spinodals and binodals with theory. We are currently focused on providing experimental evidence for these ideas. Even without evoking these conjectures, we conclude that new theories are necessary to understand phase transitions in thin film mixtures, a topic which continues to remain unsolved in spite of over 30 years of theoretical study.

Acknowledgment. Financial support was provided by the National Science Foundation, Division of Materials Research [DMR-0113756]. We thank C. Glinka for helpful discussions and Charles Han, Holger Grull, and Nitash Balsara for providing us with the polymers. We acknowledge the support of the National Institute of Standards and Technology, U.S. Department of Commerce, in providing the neutron research facilities used in this work. This work utilized facilities supported in part by the National Science Foundation under Agreement No. DMR-9986442.

References and Notes

- Binder, K.; Nielaba, P.; Pereyra, V. *Z. Phys. B* **1997**, *104*, 81–98.
- Müller, M.; Albano, E. V.; Binder, K. *Phys. Rev. E* **2000**, *62*, 5281–5295.
- Rouault, Y.; Baschnagel, J.; Binder, K. *J. Stat. Phys.* **1995**, *80*, 1009–1030.
- Reich, S.; Cohen, Y. *J. Polym. Sci., Polym. Phys. Ed.* **1981**, *19*, 1255–1267.
- Andreyeva, V.; Dolinnyy, A.; Burdin, A.; Kozhevnikova, Y. *Fluid Mech. Res.* **1992**, *21*, 72.
- Nesterov, A. E.; Lipatov, Y. S.; Horichki, V. V.; Ignatova, T. D. *Macromol. Chem. Phys.* **1998**, *199*, 2609–2612.
- Lipatov, Y. S.; Nesterov, A. E.; Ignatova, T. D.; Nesterov, D. A. *Polymer* **2002**, *43*, 875–880.
- Karim, A.; Yurekli, K.; Meredith, C.; Amis, E.; Krishnamoorti, R. *Polym. Eng. Sci.* **2002**, *42*, 1836–1840.
- Slaweki, T. Ph.D. Thesis; The Pennsylvania State University, University Park, PA, 1994.
- Akpalu, Y.; Karim, A.; Balsara, N. P. *Macromolecules* **2001**, *34*, 1720–1729.
- Steiner, U.; Klein, J.; Fetters, L. *Phys. Rev. Lett.* **1994**, *72*, 1498–1501.
- Karim, A.; Slaweki, T.; Kumar, S.; Russell, T.; Han, C.; Satija, S.; Liu, Y.; Rafailovich, M.; Sokolov, J.; Overney, R. *Macromolecules* **1998**, *31*, 857–862.
- Newby, B. Z.; Wakabayashi, K.; Composto, R. J. *Polymer* **2001**, *42*, 9155–9162.
- Grüll, H.; Schreyer, A.; Berk, N. F.; Majkrzak, C. F.; Han, C. *Europhys. Lett.* **2000**, *50*, 107–112.
- Grüll, H.; Sung, L.; Karim, A.; Douglas, J. F.; Satija, S. K.; Hayashi, M.; Jinnai, H.; Hashimoto, T.; Han, C. C. *Europhys. Lett.* **2004**, *65*, 671–677.
- Indrakanti, A.; Jones, R. L.; Kumar, S. K. *Macromolecules* **2004**, *37*, 9–12.
- Zheng, X.; et al. *Phys. Rev. Lett.* **1997**, *79*, 241.
- Zhang, Y.; et al. *Langmuir* **2001**, *17*, 4437.
- Lin, E. K.; Kolb, R.; Satija, S. K.; Wu, W.-L. *Macromolecules* **1999**, *32*, 3753.
- Silberzan, P.; Leger, L. *Macromolecules* **1992**, *25*, 1267.
- Horn, R.; Israelachvili, J. *Macromolecules* **1988**, *21*, 2836–2841.
- Montfort, J. P.; Hadziioannou, G. *J. Chem. Phys.* **1988**, *88*, 7187.
- Sukhishvili, S. A.; Chen, Y.; Muller, J. D.; Gratton, E.; Schweizer, K. S.; Granick, S. *Macromolecules* **2002**, *35*, 1776.
- Mubarekyan, E.; Santore, M. M. *Macromolecules* **2001**, *34*, 7504–7513.
- Chakraborty, A.; Adriani, P. M. *Macromolecules* **1992**, *25*, 2470–2473.
- Sternstein, S. S.; Zhu, A. J. *Macromolecules* **2002**, *35*, 7262–7273.
- Bruinsma, R. *Macromolecules* **1990**, *23*, 276.
- Dannenberg, E. M. *Rubber Chem. Technol.* **1986**, *59*, 512–524.
- Wolff, S.; Wang, M. J. *Rubber Chem. Technol.* **1992**, *65*, 329–342.
- Reiter, G.; Khanna, R. *Langmuir* **2000**, *16*, 6351–6357.
- Reiter, G. *Phys. Rev. Lett.* **1992**, *68*, 75–78.
- Jones, R.; Kumar, S.; Ho, D.; Briber, R.; Russell, T. *Nature (London)* **1999**, *400*, 146–149.
- Sakurai, S.; Jinnai, H.; Hasegawa, H.; Hashimoto, T.; Han, C. *Macromolecules* **1991**, *24*, 4839.
- Note that, in principle, the two chains have different R_G values. It is generally impossible to separately determine the radii of gyration of both species, since there are few features in the data that allow for this separation. To solve this problem, we follow the standard procedure: we use the identity, $R_G^2 = N\sigma^2/6$ and fit to one value of σ , which is then the weighted mean of the σ of the two chains.
- Müller, M. *J. Chem. Phys.* **2002**, *116*, 9930–9938.
- The q range of interest in our experiments is typically $0.0035\text{--}0.03 \text{ \AA}^{-1}$. Since the R_G of the chains is $\approx 150 \text{ \AA}$, the range of qR_G that is considered here is $\approx 0.5\text{--}5$. From the results of Müller, we can see that the error between the scattering functions derived from RPA and simulations is less than 10%, i.e., comparable to the experimental error in the estimation of $I(0)$. We thus conclude that the use of RPA is justified here.
- Schwahn, D.; Mortensen, K.; Yee-Madeira, H. *Phys. Rev. Lett.* **1987**, *58*, 1544–1546.
- Janssen, S.; Schwahn, D.; Springer, T. *Phys. Rev. Lett.* **1992**, *68*, 3180–3183.
- Flory, P. *Principles of Polymer Chemistry*; Cornell University Press: Ithaca, NY, 1953.
- Budkowski, A. *Adv. Polym. Sci.* **1999**, *148*, 1–111.
- Flebbe, T.; Dunweg, B.; Binder, K. *J. Phys. II* **1996**, *6*, 667–695.
- Sung, L.; Karim, A.; Douglas, J.; Han, C. *Phys. Rev. Lett.* **1996**, *76*, 4368–4371.
- Leibler, L.; Mourran, M. *MRS Bull.* **1996**, *22*, 33–37.
- Matsen, M. W.; Gardiner, J. M. *J. Chem. Phys.* **2001**, *115*, 2794–2804.
- Shull, K. *Faraday Discuss.* **1994**, *98*, 203–217.